Preclinical extracranial aneurysm models for the study and treatment of brain aneurysms: A systematic review

Serge Marbacher[1,2], Fabio Strange[1,2] ⓘ, Juhana Frösén[3] and Javier Fandino[1,2]

Abstract

Animal models make an important contribution to our basic understanding of the pathobiology of human brain aneurysms, are indispensable in testing novel treatment approaches, and are essential for training interventional neuro-radiologists and neurosurgeons. Researchers are confronted with a broad diversity of models and techniques in various species. This systematic review aims to summarize and categorize extracranial aneurysm models and their characteristics, discuss advantages and disadvantages, and suggest the best use of each model. We searched the electronical Medline/PubMed database between 1950 and 2020 to identify main models and their refinements and technical modifications for creation of extracranial aneurysms. Each study included was assessed for aneurysm-specific characteristics, technical details of aneurysm creation, and histological findings. Among more than 4000 titles and abstracts screened, 473 studies underwent full-text analysis. From those, 68 different techniques/models in five different species were identified, analyzed in detail, and then grouped into one of the five main groups of experimental models as sidewall, terminal, stump, bifurcation, or complex aneurysm models. This systematic review provides a compact guide for investigators in selecting the most appropriate model from a range of techniques to best suit their experimental goals, practical considerations, and laboratory environment.

Introduction

Brain aneurysms are a cerebrovascular disease in which a weakening of a cerebral artery causes an abnormal focal dilatation. Microsurgical and endovascular treatment aims to eliminate brain aneurysms from cerebral circulation and prevent rupture. Despite rapid advances in the development of endovascular treatment, complete and long-lasting aneurysm occlusion remains a challenge, and the biological mechanisms that predispose brain aneurysms to grow and recanalize are not yet fully understood.[1,2] Although strong histological similarity exists between the cerebral arteries of humans and animals, the prevalence of naturally developed cerebral aneurysms in animals is extremely low.[3,4] Models with artificial induction of aneurysm formation are therefore needed for preclinical studies of the pathobiology of human brain aneurysms as well as to

evaluate and invent novel endovascular devices and medical therapies that prevent rupture and recurrence after endovascular therapy.

Current models can be divided in two main groups: first, intracranial aneurysm models serve to evaluate induction, growth, and rupture of brain aneurysms

[1]Department of Neurosurgery, Kantonsspital Aarau, Aarau, Switzerland
[2]Cerebrovascular Research Group, Department for BioMedical Research, University of Bern, Bern, Switzerland
[3]Hemorrhagic Brain Pathology Research Group, Department of Neurosurgery, University of Tampere and Tampere University Hospital, Tampere, Finland

Corresponding author:
Serge Marbacher, Department of Neurosurgery, Kantonsspital Aarau, Tellstrasse, 5001 Aarau, Switzerland.
Email: serge.marbacher@ksa.ch

and, second, extracranial aneurysm models that are mainly designed to test novel endovascular treatment options. Animal models of intracranial aneurysm formation induced by flow manipulation, hypertension, and impaired collagen synthesis developed by Prof. Nobuo Hashimoto et al.[5] are the most physiological models in terms of reproducing human morphology, histology, hemodynamics, and brain aneurysm vessel surroundings. In all other models, including the induction of intracranial aneurysms by intrathecal elastase injection,[6] aneurysms are created by direct vessel manipulation of intra- and extracranial arteries. This review focuses exclusively on extracranial aneurysm models for the study of endovascular therapies in the most often used species, that is, mouse, rat, rabbit, dog, and swine. Extracranial animal models in sheep[7] and monkey[8,9] have also been described but have never undergone detailed methodological analysis and are seldom used today.

Although the number of studies using animal aneurysm models has steadily increased in recent years, no model has yet been established as the generally accepted standard for preclinical testing.[10,11] To the contrary, confronted with a diversity of animal models and techniques, investigators now face increasingly complexity in choosing the appropriate model for any given research question. Specifically, endovascular technology is progressing rapidly, traditional surgically constructed models have been adapted, and novel models and techniques have been designed. This review aims to provide a contemporary detailed overview of available extracranial aneurysm models and discusses advantages and disadvantages of specific species and techniques.

Materials and methods

Search strategy

The literature was reviewed to identify main animal models of experimental saccular aneurysm, their refinements, and technical modifications. We searched the database Medline/PubMed on 10 January 2020 using the key words "mouse," "rat," "rabbit," "dog," and "swine" in combination with "aneurysm" with the Boolean operator (AND). The search was restricted to "animals." Two investigators (SM and FS) independently screened titles and abstracts for eligibility based on our predefined criteria, reviewed the full text of eligible studies, and confirmed articles for inclusion. Any disagreement about a particular study's eligibility was resolved with consensus of the other authors. Additionally, we identified studies cited in previous reviews and added select articles by cross-reference checking until no other publications were found.

Figure 1 outlines the applied search algorithm applied and reasons for exclusion in accordance with the Preferred Reporting Items for Systematic Reviews and Meta-Analyses (PRISMA) guidelines.[12]

Eligibility criteria and analyzed features

We considered in vivo extracranial aneurysm models in mice, rats, rabbits, dogs, and swine but excluded non-English publications and studies on intracranial aneurysms. In the rare case of a model in which an extracranial vessel was transposed or transplanted into the intracranial space, the model was, despite its anatomical location, assessed as an extracranial aneurysm model. For each included study, we recorded authors; year of publication; detailed technique of aneurysm creation; number of created aneurysms; time for creation; patency rate; histological findings; mortality and morbidity; and shape, size, and location of the aneurysms.

Animal models were defined with consideration to the large differences that occur in the natural course of aneurysms among species. Therefore, we considered the animal model to be unique when identical techniques of aneurysm induction were performed in either different species or a different anatomical location within the same species or with any variation in the aneurysm graft (arterial or venous pouch) or with modification by chemical or mechanical means. Besides differences in species, anatomical location, or graft characteristics, a model was defined as novel only if modifications of an existing technique were major, that is, resulting in significant changes in aneurysm size or shape, patency rate, time for creation, or morbidity and mortality. Any uncertainty about the novelty of a particular study was resolved by two authors based on the predefined criteria listed above.

Results

From 4295 publications related to the main animal models of experimental saccular aneurysm, including refinements and technical modifications, our further screening of titles and abstracts and removal of duplicates identified 473 studies for detailed full-text analysis. Among these, a total of 68 techniques were found that included mice (n = 4), rats (n = 16), rabbits (n = 19), dogs (n = 23), and swine (n = 6). For each technique, details of the animal model, localization, time for creation, size of the aneurysm, patency rate, and morbidity and mortality are outlined in Supplementary Tables. We defined five main groups of aneurysm models as (1) sidewall, (2) terminal, (3) bifurcation stump, (4) natural and artificial bifurcation, and (5) complex aneurysm models (Figure 2).
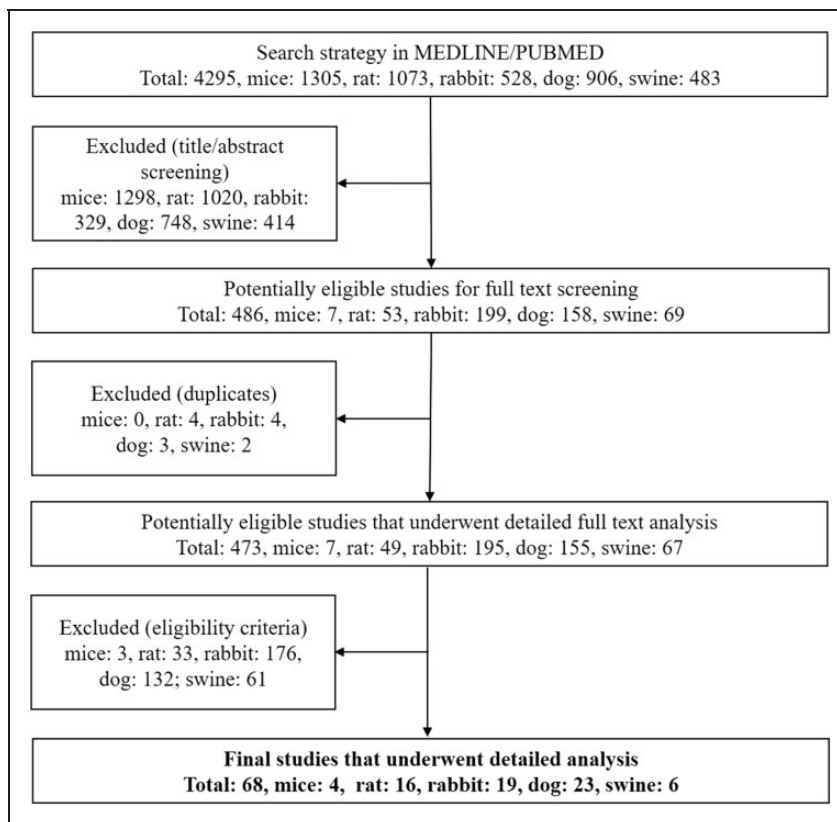
Figure 1. PRISMA flowchart of PubMed search strategy and selection process. Among more than 4000 titles and abstracts screened, 473 studies underwent detailed full-text analysis. From those, 68 models, including refinements and technical modifications, were identified in five different species.

In these aneurysm models, aneurysm walls consisted of either a venous or an arterial vessel segment (autogenic and allogenic grafts). Creation was performed surgically, by inducing vessel wall weakening (chemical or physical), or a combination of both. Methods to weaken the vessel walls consisted of treatment with elastase, papain, collagenase, $CaCl_2$, or sodium dodecyl sulfate; mechanical destruction (e.g., arteriotomy) followed by laser sealing or glue application; or mechanical transluminal or external destruction of various parts of the vessel wall. Among all species, aneurysms were created in anatomical locations that included the femoral artery, common iliac artery, external and internal iliac artery, aortic bifurcation, abdominal aortic artery, renal artery, brachiocephalic artery, subclavian artery, vertebral artery, common carotid artery (CCA), CCA bifurcation, ascending cervical artery, external carotid artery (ECA), ascending pharyngeal artery, lingual artery, maxillary artery, superior thyroid artery, ascending cervical artery, basilar artery, and middle cerebral artery (Figure 3), respectively. Subtypes of these models are given in Figures 4 and 5, and their method depicted in step-by-step illustrations (Supplementary Figures).

Compared to dogs and pigs, smaller animals such as mice, rats, and rabbits have the advantages of lower costs and easier handling. Although not all endovascular devices can be tested in mice and rats, transgenic animals are widely available and immunohistochemical and molecular biology techniques are easier to apply. Unlike all other species, pigs show an unfavorable strong tendency for spontaneous thrombosis and excessive healing reaction. Sidewall, untreated stump, and natural bifurcation models are the simplest and quickest techniques for creating extracranial aneurysms. In contrast, the terminal, artificial bifurcation, treated stump, and complex models are resource intensive, surgically demanding, and time-consuming. The sidewall model allows creation of most standardized aneurysm shapes with good reproducibility. However, the hemodynamic condition differs significantly from most human aneurysms. Artificial bifurcation and complex models exhibit comparably worse reproducibility but do allow for great variability in aneurysm shape and have flow characteristics like those seen in human aneurysms. Advantages and disadvantages of each animal and the five main extracranial aneurysm models are summarized in Tables 1 and 2.
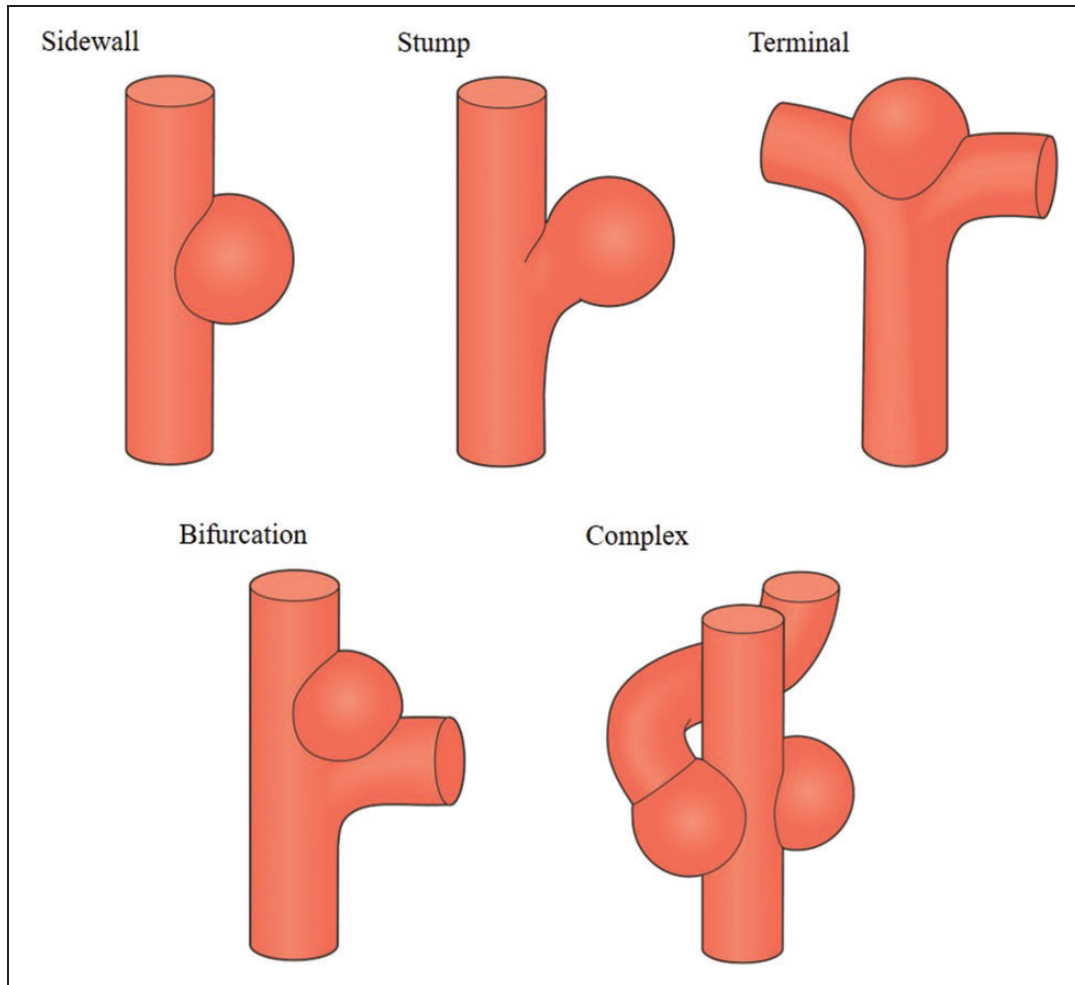
Figure 2. Main groups of extracranial aneurysm models. Preclinical extracranial aneurysm models in different species can be categorized into one of the five main groups. Top form left to right: (1) sidewall aneurysm models, (2) bifurcation stump aneurysm models, and (3) terminal aneurysm models. Down from left to right: (4) natural and artificial bifurcation aneurysm models and (5) complex aneurysm models.
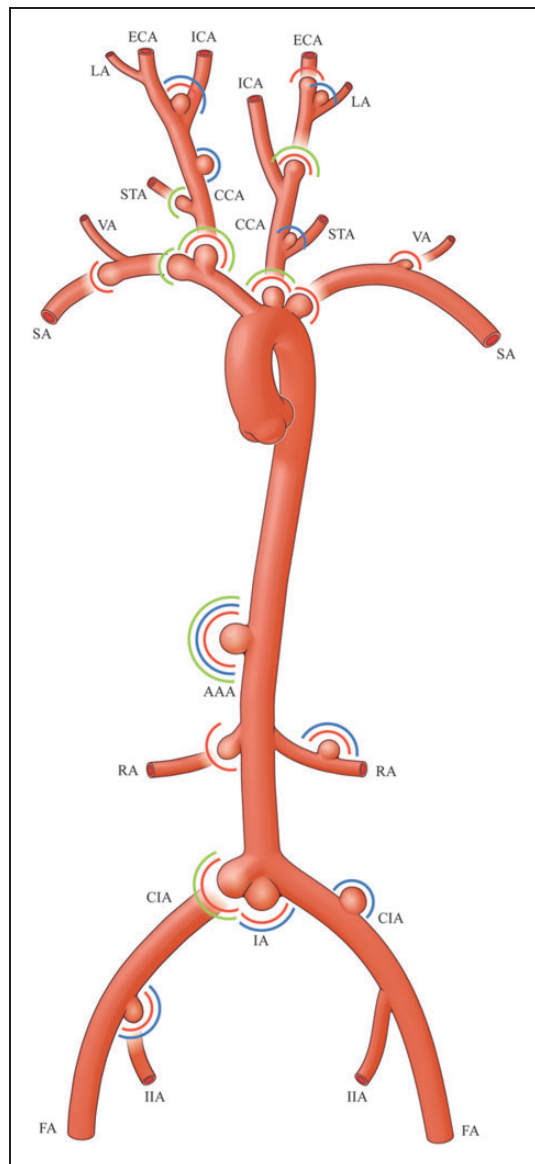
Sidewall aneurysm model

The sidewall aneurysm model, described by German and Black, is the oldest microsurgical technique to produce experimental aneurysms (Figure 4, A1).[13] The two variations of this technique have used (1) an isolated vein graft sutured end-to-side onto the parent artery (Supplementary Figure A1A) and (2) an arteriovenous fistula created by end-to-side or side-to-side suturing of a vein onto the parent artery followed by immediate or delayed ligation of the fistula (Supplementary Figure A1B).[14,15] Modifications include weakening of the parent artery with the use of nitrogen mustard, elastase, or mechanical destruction and subsequent aneurysmal outpouching at the site of the damaged vessel segment. Although the size of arteriotomy can be standardized, the size of the venous pouch itself and ultimately the aneurysm volume varies greatly. Only use of

an arterial graft can ensure the standardization of aneurysm size.

To date, the most standardized aneurysm model in terms of graft origin, aneurysm shape and dimensions, volume-to-orifice ratio, and parent vessel to aneurysm long axis angle is the rat sidewall aneurysm created by an arterial pouch (Figure 4, A2; Supplementary Figure A2).[16] The patency rate of sidewall aneurysms depends to a large extent on the animal used. Untreated sidewall swine aneurysms have a tendency for spontaneous thrombosis.[17–19] Unlike the tendency for spontaneous thrombosis in swine,[17–19] the sidewall venous pouch aneurysm models in the rat, rabbit, and dog achieved excellent rates of long-term patency, that is, 100% (84/84),[16] 95% (38/40),[20] and 94% (81/86),[21] respectively, without need for an antithrombotic regimen.

Figure 3. Anatomical locations of extracranial aneurysm models. Green circle: modified pouch; blue circle: venous pouch; red circle: arterial pouch. AAA: abdominal aortic artery; CCA: common carotid artery; CIA: common iliac artery; ECA: external carotid artery; FA: femoral artery; IA: iliac artery bifurcation; ICA: internal carotid artery; IIA: internal iliac artery; LA: lingual artery; RA: renal artery; SA: subclavian artery; STA: superior thyroid artery; VA: vertebral artery.
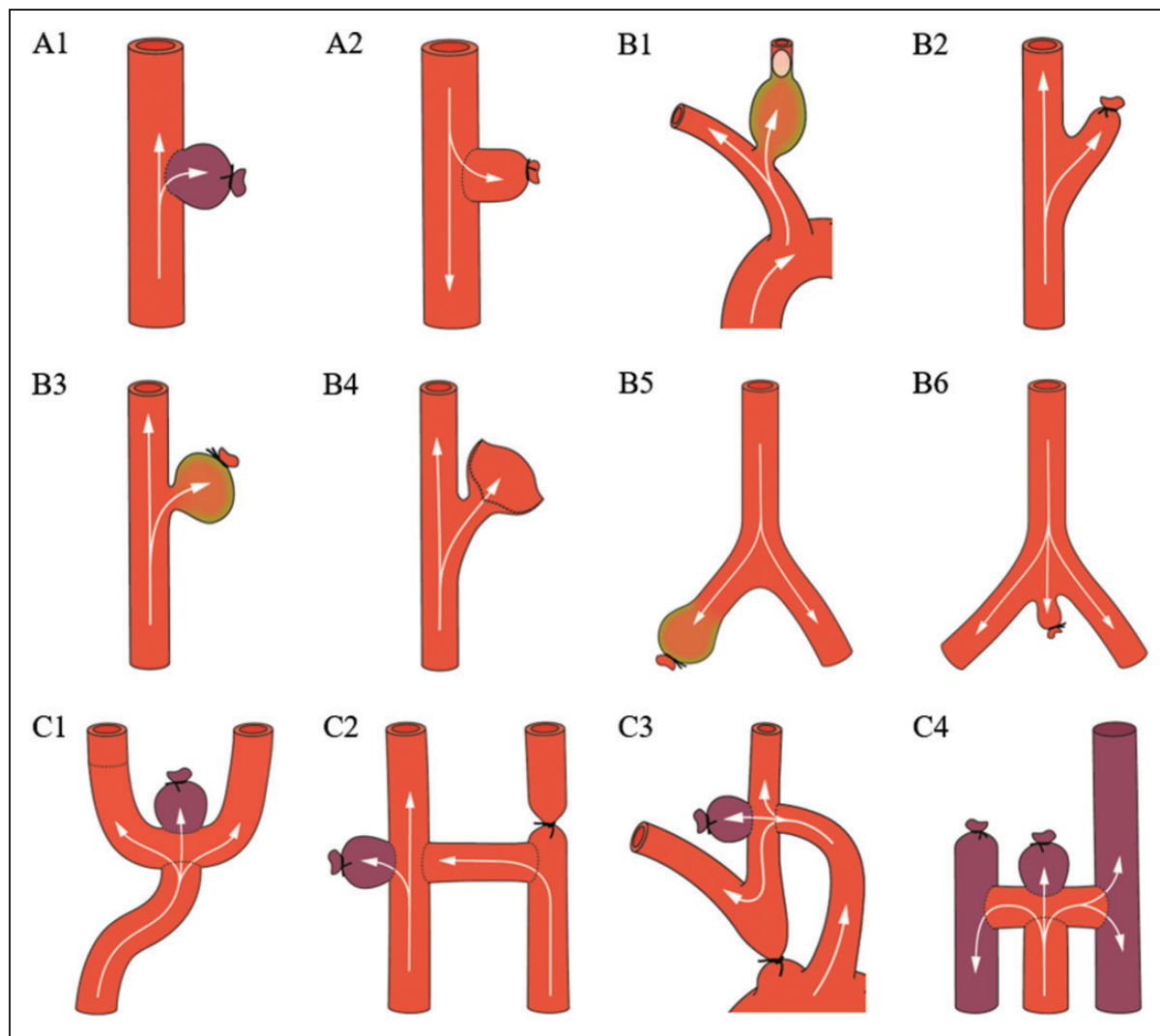
Stump aneurysm model

Fingerhut and Alksne[22] were among the first to ligate a major muscular branch of the femoral artery to create an arterial stump. Unlike all other bifurcation stumps, the tail artery stump in dogs (abdominal aortic trifurcation), described by Roach,[23] represents a natural arterial bifurcation (Figure 4, B6; Supplementary Figure B6). Following these original descriptions, others have reported untreated arterial stump models

at different anatomical locations and in various species. Untreated stumps are the simplest, fastest method to create an arterial pouch (even in relatively small species) and therefore are ideal models to screen potential embolization materials (Figure 4, B2; Supplementary Figure B2).[24–26]

Influenced by previous experimental work of elastase-induced abdominal aortic aneurysms in rats,[27] Cawley et al.[28] infused elastase (via microcatheter from the femoral artery) into unilateral and bilateral surgically created stumps of the ECA in rabbits (Figure 4, B3; Supplementary Figure B3). Cloft et al.[29] elaborated on a purely endovascular-based arterial aneurysm model. After blocking the origin of the left CCA 2 cm distal to the vessel origin using a detachable balloon, they infused the stump with elastase for 30 min (Figure 4, B1; Supplementary Figure B1). Altes et al.[30] modified a version of this model that reduced creation time (<1 h) and procedural morbidity and mortality. They surgically exposed the right CCA, blocked its origin retrograde with a pliable balloon, and infused the distal stump with elastase. The group proposed several modifications to their right CCA model to customize resultant aneurysm morphology.[31–33] Because the right CCA model is more of a sidewall-type aneurysm (origins as bifurcation from the subclavian artery), Ding et al.[34] adapted their previous modifications to the left CCA (originates as a trifurcation between the brachiocephalic artery and aortic arch) to create a more bifurcation type elastase-induced aneurysm in 2013.

Others proposed improvements for the elastase-induced CCA bifurcation stump model. Krings et al.[35] advocated fluoroscopic guidance of elastase infusion to prevent leakage into aberrant tracheal arteries in effort to reduce mortality and morbidity (mainly attributed to hemorrhagic necrosis of the trachea).[36] One year later, Hoh et al.,[37] also concerned by reports of failure of the original model due to aberrant branches from the right CCA,[38] proposed temporary clip placement at the origin of the right CCA and infusion of the lumen under visual control (aberrant branches are ligated or coagulated). The technique reduced procedure time by 35 min, eliminated the need for fluoroscopy, and minimized the use of endovascular supplies. More recently, Kainth et al.[39] proposed to ligate the left or right CCA 4–6 mm distal to the bifurcation, precisely brush the apex of the blind pouch using a 10/0 round-tip paint brush, and anchor the aneurysm to influence its orientation. This extravascular elastase application supposedly eliminates the need for angiography and endovascular supplies, preserves the femoral arteries for follow-up imaging or endovascular procedures, and allows for variation in

Figure 4. Sidewall, stump, and terminal aneurysm models. Sidewall aneurysms are created by suturing either a venous (A1) or arterial (A2) unmodified pouch onto a parent artery. Stump aneurysms are created by endovascular occlusion, ligature, or flap construction of a branching artery (B1–B5). Modification of the aneurysm wall (green) allows for growth of the stump into a more saccular shape. The tail artery stump represents a unique true arterial bifurcation model (B6). Terminal aneurysm models are designed to simulate flow conditions similar to human basilar and internal carotid artery bifurcation aneurysms (C1–C4).

the orientation of the aneurysm relative to the parent vessel.

The elastase-induced ECA bifurcation stump model also underwent modifications. Wang et al.[40] proposed to ligate the ECA temporally using an aneurysm clip and infuse the ECA stump with elastase for 20 min. This surgical procedure is simple, fast, and requires no interventional support. Elastase-induced bifurcation stump models have also been introduced in the right[41] and left[42] CCA in mice and in the abdominal aortic bifurcation in rats.[43]

The original elastase-induced right CCA bifurcation stump model in rabbits is one of the best characterized saccular aneurysm models. Serial angiography on days 1, 3, 5, 7, 14, and 21 demonstrated progressive enlargement, but thereafter the aneurysm size remained stable on one, two, three, and four months imaging.[44] An excellent long-term patency of 92% was confirmed in a five-year follow-up study.[45] Mortality rates associated with aneurysm creation and the embolization procedure were 8.4% (59/700) and 8.1% (43/529), respectively.[46] Hemodynamic analysis revealed that most features of the elastase-induced right CCA model are qualitatively and quantitatively similar to many of human cerebral aneurysms.[47] In a dose-escalation study, native bifurcation stumps failed to create saccular aneurysms.[48] However, increased elastase concentration or incubation time or both
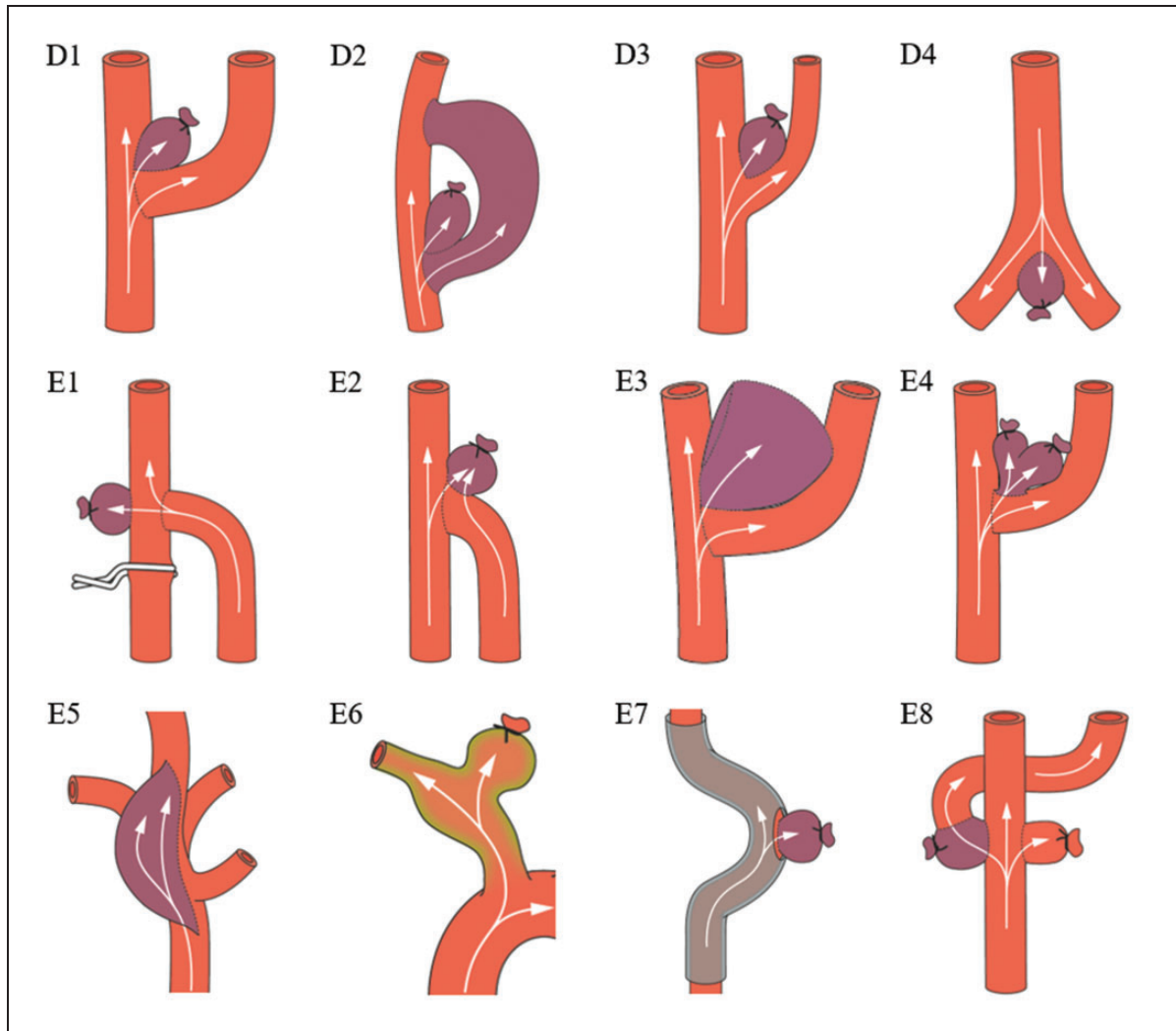
Figure 5. Bifurcation and complex aneurysm models. Bifurcation aneurysms are created by suturing a venous pouch into an artificially created bifurcation (D1 and D2). A natural bifurcation aneurysm model is created when a venous pouch is sutured into an already existing bifurcation (D3 and D4). Complex aneurysm models comprise a heterogenous group of microsurgically created aneurysms that mimic rare forms of intracranial aneurysms such as confluence (E1 and E2), giant sized (E3), multilobulated (E4), fusiform (E5 and E6), curved (E7), or aneurysms with a side branch (E8).

demonstrated a trend for widening parent arteries but did not result in larger aneurysms cavities at three weeks follow-up. Rather, the aneurysms were mainly caused by the initial infusion of elastase and not by ongoing wall remodeling and degradation by endogenous proteases.[49] Nevertheless, histological analysis has demonstrated that this model mimics wall types that have been identified in human intracranial aneurysms.[50,51]

Terminal aneurysm model

Terminal aneurysms are aimed at simulating human basilar tip and internal carotid artery (ICA) bifurcation aneurysms. Originally described by Strother et al. in 1992, they were constructed by forming an arch with end-to-end anastomosis of both CCAs (Figure 4, C1; Supplementary Figure C1).[52] One should be aware that the volume increases as the aneurysm matures during the first few weeks but thereafter remains stable (up to six months follow-up).[53] With its distinctive hemodynamic stress, terminal aneurysms demonstrate 100% patency in rat (9/9)[54] and rabbits (9/9)[55] and 85% to 100% (11/13)[56] to (16/16)[53] in dogs. Even in swine where long-term patency is a concern, terminal aneurysms have been reported to have direct intraluminal blood flow with a 100% (3/3) patency rate at three-month follow-up.[19]

Table 1. Advantages and disadvantages of each animal.

Animal	Advantages	Disadvantages
Mice and rats	-Low costs, widely available -Reliable anesthesia -Readily applied immunohistochemical and molecular biological techniques -Ethically acceptable -High aneurysm patency rates without the need for anticoagulation in most models -Availability of transgenic animals -Allows for a larger number of experiments and subsequently increased statistical power	-Limited access for diagnostic and interventional catheterization -Although small stents and coils are applicable ins some models, not all endovascular devices can be tested (size-related) -Requires microsurgical expertise particularly operation on the carotid arteries (small vessel size)
Rabbits	-Relatively low costs, wide availability -Easy handling (nonaggressive behavior) -Carotid artery diameter comparable to human major cerebral arteries -Similarities to hemodynamics, thrombosis, and thrombolysis seen in humans -Readily access to diagnostic and interventional catheterization -Well-characterized models (especially the carotid artery elastase-induced bifurcation stump model)	-Relatively high perioperative morbidity and mortality (anesthetic-related death, long-term housing complications, respiratory infections) -Challenging anesthesia and endotracheal intubation -Some groups advocate anticoagulant therapy for patency of some models
Dogs	-Active fibrinolytic system with high patency rate, no need for anticoagulation -Readily access for diagnostic and interventional catheterization -Suitable for testing endovascular devices of all sizes -Well-characterized models -Reliable anesthesia	-Ethical concerns -Require veterinary anesthesiologist -High costs for care and housing -Restricted availability
Swine	-Readily access for diagnostic and interventional catheterization -Suitable for testing endovascular devices of all sizes -Well-established models -Reliable anesthesia	-Abandoned healing reaction -Tendency for spontaneous thrombosis -Require veterinary anesthesiologist -High costs for care and housing

Bifurcation aneurysm model, natural, and artificial variations

Natural bifurcation aneurysm model. Stehbens first created a natural bifurcation aneurysm model in rabbits by suturing a venous pouch into the bifurcation of the abdominal aorta (Figure 5, D4; Supplementary Figure D4A).[57] Ujiie et al.[58] modified the arteriotomy and venous pouch ligature to achieve narrow or broad-based aneurysms shaped as dumbbell, oval, and lobular. In delivering elastase topically to the bifurcation of either the right CCA or the right superior thyroid artery bifurcation, Miskolczi et al.[59] found that aneurysm formation was mainly at the latter location. Nishikawa et al.[60] and Young et al.[61] induced natural bifurcation models in rats by suturing a vein pouch or inducing external damage to the vessel wall at the site of CCA/ECA bifurcation.

Since mechanical destruction at the apex of the CCA/ECA bifurcation from the outside failed to produce aneurysmal bulging, it was concluded that the internal elastic lamina represents a critical structure in aneurysm formation.[62] Accordingly, van Alphen et al.[63] achieved aneurysm formation in rats by transluminal (via arteriotomy proximal to the CCA/ECA bifurcation) removal of the tunica intima and media. Mucke et al.[64] harvested a CCA vessel segment and sutured this arterial graft into the aortic bifurcation in rats (Supplementary Figure D4B). In dogs, Sekhar et al.[65], Macdonald et al.[56], and Shin et al.[66] created an aneurysm by suturing a venous pouch in the natural bifurcation between the CCA and superior thyroid artery, lingual artery, and cranial thyroid artery, respectively (Figure 5, D3; Supplementary Figure D3). Boulos et al.[67] used the ECA-lingual artery bifurcations to create bilateral aneurysms. In swine, Massoud et al.[68] created natural bifurcation aneurysms at the CCA-ascending pharyngeal artery.

Table 2. Methods of aneurysm creation: Advantages and disadvantages of main models.

Model	Advantages	Disadvantages
Sidewall	-Fast and technically easy aneurysm creation -Multiple aneurysms in one animal -Control and experimental arm in one animal possible (e.g., both carotid arteries) -Standardized aneurysm shapes and volumes, good reproducibility -High rates of long-term patency in rats, rabbits, and dogs without need for anticoagulation therapy	-Hemodynamic condition differs significantly from most human aneurysms -High rate of thrombosis in swine -Surgical trauma at the artificial aneurysm neck
Stump (untreated)	-Fastest and easiest way to construct an aneurysm -Low costs (no additional catheter/deployment or suture material) -Multiple aneurysm in one animal -Control and experimental arm in one animal possible (e.g., both carotid arteries) -Highly standardized aneurysm shapes and volumes, excellent reproducibility -Ideal for screening (embolization material) in smaller animals	-Unfavorable hemodynamic condition with most models (except for the tail artery stump which represents a natural bifurcation)
Stump (treated)[a]	-Fast and technically easy aneurysm creation (when modifications of original model are applied) -Standardized aneurysm shapes and volumes, good reproducibility -No microsurgical skills required -Excellent long-term patency without need for anticoagulation therapy -No micro anastomosis -Healing (rate of recurrence) comparable to that seen in humans	-Need for sophisticated laboratory equipment (less demanding when modifications of original model are applied)
Terminal	-Specific flow conditions such as human terminal internal carotid artery or basilar tip aneurysms -High patency rates in all species (even in swine)	-Need for microsurgical skills and sophisticated laboratory equipment -Only one aneurysm per animal -Unknown biological effect of artery wall disruption and surgery at the site of micro anastomosis
Bifurcation (artificial)	-Flow dynamics as those in natural bifurcation aneurysm models and most human aneurysms -Shape and size highly variable -High patency rates in all species (even in swine) -Healing (rate of recurrence) comparable to that seen in humans	-Need for microsurgical skills and sophisticated laboratory equipment -Only one aneurysm per animal -Unknown biological effect of artery wall disruption and surgery at the site of micro anastomosis -Great variability of shape and size with most methods, poor reproducibility -Associated with a learning curve and initial long procedural times
Bifurcation (natural)	-Favorable hemodynamics -Easier and faster to construct than an artificial bifurcation -When constructed in the neck two aneurysms per animal possible -Lower tendency to thrombose when compared with sidewall aneurysm	-Surgical trauma at the artificial aneurysm neck -Requires microsurgical skills and the requisite laboratory equipment (microscope)
Complex	- Allows creation of aneurysms with complex shape and large to giant size -Angioarchitecture (parent artery configuration) highly variable (curved sidewall, confluence, and fusiform aneurysm models with or without side branches) -Allows to test novel endovascular devices in highly specific narrow conditions	-Often need for long operation duration, high microsurgical skills and sophisticated laboratory equipment (some models even require two surgeons to create) -Only one aneurysm per animal in most models -Poor reproducibility in some models

[a]Advantages and disadvantages mainly relate to the right common carotid artery elastase bifurcation stump aneurysm model.

Artificial bifurcation aneurysm model. Forrest and O'Reilly were the first to create an artificial bifurcation aneurysm by suturing a venous pouch into the end-to-side anastomosis of the left to right CCA in rabbits (Figure 5, D1; Supplementary Figure D1).[69] Despite an excellent 97% patency rate (34/35) at 1–10 weeks follow-up, the 22% morbidity rate (10/45) was rather high. Subsequent modifications of the surgical technique (i.e., preservation of laryngeal nerves, tensionless anastomosis, reduction of number of sutures and procedural time) and improved anticoagulation and peri- and postoperative management successively reduced the mortality/morbidity rate from 24%,[70] <20%[71] to 0%[72] and maintained high patency rates (100%[71] and 87.5%[72]) at one-month follow-up.

Creation of such aneurysms requires profound microsurgical skills. Accordingly, operative times decreased during the experimental series (from 210 to 90 min[71] and from 225 to 115 min[72]). The same venous pouch technique for artificial bifurcation aneurysms performed at the same location in the rat, dog, and swine species achieved excellent patency rates (100% in 12/12).[73]

Complex aneurysm model

This group represents microsurgically created aneurysms that mimic rare forms of intracranial aneurysms such as giant sized, broad-based, no-neck, fusiform, blister-like, bisaccular, bi- or multilobular, or confluence artery aneurysms. Nishikawa et al.[74] had already reported confluence aneurysms in dogs by inclusion of a vein graft into an intracranial lingual-basilar artery anastomosis. Jiang et al.[75] designed a dog confluence aneurysm model that used both the CCA and a vein graft to closely mimic human vertebral confluence aneurysms (Figure 5, E2; Supplementary Figure E2). Complex shaped bilobular, bisaccular, and broad-neck microsurgical aneurysms were created using various combinations of vein grafts in the rabbit artificial bifurcation model (Figure 5, E4; Supplementary Figure E4A–E4C).[76] Despite the complex angioarchitecture, the aneurysms proved excellent long-term patency.[77]

Varsos et al.[14] first attempted to create a giant aneurysm by inducing a fistula between the CCA and external jugular vein and ligating this fistula one week later to form a giant sidewall aneurysm pouch (Supplementary Figure E3B). Yapor et al.[78] presented a modification with a one-stage approach (Supplementary Figure E3C). Almost two decades later, giant aneurysms (approximately 1×2.5 cm) were created in the canine terminal[79] and rabbit artificial bifurcation[80] models (Supplementary Figure E3A).

With the emergence of novel endovascular technologies that extended the indications for treatment to a broader range of intracranial aneurysm (IA) morphologies, new preclinical models were needed. More recently fusiform[81] and curved sidewall[82] aneurysm models were designed in rabbits and dogs. Darsaut et al.[83] introduced a giant fusiform model that used a rhomboid venous patch sutured to the anterior aspect of the lingual artery that allowed testing of flow diverters (Figure 5, E5; Supplementary Figure E5A).

Based on this groundwork, Greim-Kuczewski et al.[84] proposed to surgically include a venous patch as a sidewall aneurysm to mimic some morphological aspects of human intracranial dysplastic, fusiform, and blood blister-like aneurysms (Supplementary Figure E5B). To test flow diverter treatment of aneurysms with side branches, Darsaut et al.[85] created complex terminal aneurysms that featured a side branch originating from the aneurysm sac (Figure 5, E8; Supplementary Figure E8). Similarly, Fahed et al.[81] created a complex fusiform rabbit aneurysm model that permitted more comprehensive testing for flow diverters (Figure 5, E6; Supplementary Figure E6). Avery et al.[86] presented a refined fusiform aneurysm model by periarterial application of combined elastase and $CaCl_2$ in a rabbit CCA. Yan et al.[87] and Nakayama et al.[88] created canine CCA curved-artery models (Figure 5, E7). First, they printed artificial hollow tortuous tubes (based on human ICA stereolitography data) and then transposed the animal's CCA into this hollow rod (Supplementary Figure E7A-C).

Complex aneurysm models uniquely address a very narrow research questions about a specific aneurysm shape or flow condition. To date, these models are typically technically difficult, time-consuming to create (some even require two surgeons[79]), and are not well standardized or characterized.

Discussion

Our systematic review confirms the great variety in vivo extracranial aneurysm models used for a range of applications from basic biological concepts to screening of endovascular materials to final testing of endovascular devices for human application. After screening more than 4000 potential publications, the 68 studies included in this review represented five major groups of extracranial animal models and techniques. Our results highlight each model's evolution and, in recent years mainly, the modifications and refinements that improved morbidity and mortality rates, reduced operation time, improved patency rates, and kept pace with the implementation of novel endovascular techniques and devices (broadened clinical indications).

An ideal extracranial aneurysm model would require the following features: (1) size of aneurysm and parent

artery similar to larger cerebral arteries (enables realistic microcatheter interventions), (2) long-term patency of the aneurysm complex without spontaneous thrombosis and no need for anticoagulation or anti-aggregation therapy, (3) standardized method with good reproducibility for comparison of treatment strategies, (4) hemodynamics, coagulation profiles (clotting and thrombolytic system), and tissue and immunologic reactions similar to those of human IA, (5) wide availability of the animal and easy handling, (6) low costs, and (7) surgical or endovascular creation technique that is simple, fast, and associated with a gentle learning curve.[89–92] None of the identified preclinical extracranial aneurysm models that are currently available combine all these ideal characteristics. In contrast with intracranial aneurysm models where aneurysms develop in cerebral arteries without direct vessel manipulation, creation of extracranial models always requires a vascular injury. Researchers should be aware of the differences in vascular biology and hemodynamic characteristics between intra- and extracranial arteries. Furthermore, extracranial aneurysms are surrounded by cell-rich connective tissue and the aneurysm wall histology differs greatly from their intracranial counterparts.

Localization

The perianeurysmal space differs greatly between that of extracranial models and human brain aneurysms. With few exceptions, aneurysms models are not created in the subarachnoid space but in the soft tissues of the mediastinum,[29,30] neck,[28,93] leg,[22,94] retroperitoneal space[58,95] or within the abdominal cavity.[96,97] Nishikawa et al. created an intracranial sidewall aneurysm by suturing an autologous vein graft aneurysm onto the main branch of the middle cerebral artery (via transzygomatic approach),[60] and sidewall and arterial confluence aneurysms were formed on the basilar and lingual arteries (via a transclival approach) in dogs.[74] O'Reilly et al.[98] relocated a rabbit vein pouch aneurysm via polyvinyl tubing from the right CCA into the subarachnoid space. However, technical difficulties, high mortality, and low patency rates prevented the further use of these techniques.

All other microsurgically created aneurysm models are surrounded by tissue that might affect intraluminal thrombosis and the healing response. The peritoneal cavity has the advantage of being less restrictive than the neck or other subcutaneous regions. Therefore, this region will potentially allow an aneurysm to grow if the wall is weakened. One specific advantage of aneurysm location on the renal artery is the possibility to control for potential ischemic embolic complications by post-mortem assessment of renal infarction.[95] Besides the

location of aneurysm creation, one must also consider the diameter of parent arteries. Comparable to the diameter of great cerebral arteries where most human brain aneurysms are located is the size of the CCA in rabbits and the abdominal artery in rats.

Creation time

The simplest and fastest surgical techniques are the sidewall, bifurcation stump, and natural bifurcation models; these take 30–60 min for creation based on whether the aneurysm pouch needs additional modification. In comparison, terminal and artificial aneurysm models need up to 3 h for creation. The most demanding and time-consuming are complex aneurysm models, which require advanced microsurgical skills, an operating microscope, and occasionally two operators to create.[79]

Costs

Small experimental animals, such as mice and rats, are associated with lower costs than larger animals that require specialized experimental equipment, anesthesia, postoperative care, and housing. Additionally, surgery on small animals eliminates the need for a veterinary anesthesiologist and costs less for animal purchase, surgery, postoperative care, and housing. Surgery can usually be performed in the research laboratory, and general anesthesia is easily maintained by the operator with non-inhalational methods. Dogs and swine are the most expensive experimental animals. Operations are usually performed under costly general inhalational anesthesia by a veterinary anesthesiologist and additional technical assistants and must be performed in a designated animal operating theater.

Patency rate

Long-term patency without spontaneous thrombosis is a key characteristic and concern of any aneurysm model. Large series in rats, rabbits, and dogs demonstrated patency rates of 92.5%,[96] 95%,[99] 94%,[21] respectively, in 90° angle sidewall aneurysm models without any anticoagulation. However, when considering these excellent patency rates achieved by experienced researchers, it remains a matter of debate to what extent other factors are important measures in preventing thrombosis. These include extensive microsurgical training and associated technical factors (suture line, vein valves, badly placed sutures, or constricted aneurysm neck),[100,101] shape and size of arteriotomy,[98] aneurysm volume-to-neck ratio,[102] angle to long axis of grafted venous pouches,[103] number of sutures, tensionless anastomosis, and perioperative and postoperative management (compensation for

fluid loss, pain management, antibiotics, vitamin complexes).[71,72] In rats and dogs, patency rates are better in artificial bifurcation models than in sidewall aneurysm models.[21,60,74] In dogs and swine, terminal aneurysm models exhibited better patency than sidewall aneurysm models.[19,56,66]

Anticoagulation

Although most groups use local irrigation of parent arteries and storage of grafts in heparinized saline, systemic application of systemic anticoagulant[58,80,104] or antiplatlet[39,75,76] drugs is also common. In a rare direct comparison of effect of systematic antiplatelet medication on the patency rate of venous sidewall CCA aneurysms in dogs, Kerber and Buschman observed greater success with aspirin than without; patency rates were 74% versus 45%, respectively, but the difference was not statistically significant.[100] Excellent long-term patency rates in large series of sidewall, terminal, bifurcation stump, and arterial bifurcation models in rat, rabbit, and dog provide evidence against the use of systematic anticoagulation. One must be especially careful with the administration of aspirin because of its potential influence on aneurysm wall biology and recurrence after endovascular therapy.[105,106]

Histopathology and aneurysm healing

Debate continues about whether the morphological and histological characteristics of human cerebral aneurysms are more accurately modeled by elastase-digested arterial stump models or by surgically created vein or arterial pouch aneurysms.[51,107] Nonetheless, there is consensus that models with a strong tendency for spontaneous thrombosis and excessive neointima formation are inappropriate for study of healing after embolization. Sidewall aneurysms (especially in swine) have demonstrated favorable healing reactions after coil embolization compared to artificial bifurcation models.[108] However, bifurcation models may also demonstrate healing rates that far exceed those seen in human aneurysms after coil embolization.[109] Recent research revealed that aneurysm healing and recurrence after endovascular treatment also depend on the aneurysm wall condition.[1,110–112] Therefore, models that depict various types of wall conditions will gain interest and become appropriate models for testing novel endovascular therapies.[50,110]

Reproducibility

Standardized and reproducible aneurysm creation is vitally important to improve preclinical assessment of novel endovascular devices and enhance comparability of results between laboratories. To date, the most standardized aneurysm models in terms of graft origin, aneurysm shape and dimensions, volume-to-orifice ratio, and parent vessel to aneurysm long axis angle are created by an arterial pouch.[55,96] To a certain degree, neck size and aneurysm volume can also be controlled and adjusted in elastase-induced aneurysms[31,33,113,114] and modified techniques have achieved more consistent/standardized aneurysm diameters.[32] In venous pouch aneurysm techniques (especially complex models), the angioarchitecture (size, shape, and flow condition) is less standardized. However, the heterogeneity of aneurysm angioarchitecture increases the external validity of the model. Therefore, both are indispensable: standard models can test and refine the basic characteristics of a novel endovascular device, whereas models with high aneurysm variability can provide more exacting tests.

Ethical considerations

Depending on the location, most sidewall and some bifurcation stump and natural bifurcation models allow for the creation of two or more aneurysms in the same animal. Such models not only reduce the overall number of animals needed but also allow testing of two treatment modalities side-to-side within a single animal. Except for a three- and four-aneurysm dog model, most artificial bifurcation and complex aneurysm models allow creation of only one aneurysm per animal.[66,67,76,79] Some aneurysm models depend on syngeneic grafts, that is, using two animals to produce one aneurysm.[16,61,96] In contrast, aneurysm models with simple and fast aneurysm creation facilitate research with a larger number of experiments, thus ensuring adequate statistical power with increased significance and ultimately fewer animals. With the exception of some historical models and thanks to modified techniques over the past decades, currently used aneurysm models harbor low rates of morbidity and mortality.

Limitation of the study

Despite systematic approach by following the PRISMA guidelines and two investigators who independently screened the literature, this review might not be exhaustive based on our inclusion and exclusion criteria. Especially in the case of recognition of a new model related to a major modification of an existing technique, we cannot exclude a certain arbitrariness in the selection process despite strict application of predefined criteria.

Taking the potential confounding effects of the chosen species and techniques into consideration, basic biological concepts of novel intracranial

aneurysm therapies can be tested in a great variety of models available today. Our categorization of models into five main groups and discussion of advantages and disadvantages allows a quick and comprehensive insight into the field. Detailed submodel analysis facilitates prediction of specific aneurysm model characteristics and therefore supports researchers in study planning, the execution of experiments, and interpretation of the results.

In summary, this systematic review of PubMed database, covering the period between 1950 and 2020, identified five main models of extracranial saccular aneurysms in mice, rats, rabbits, dogs, and swine, and their subsequent refinements and technical modifications. This review may serve as a compendium for investigators to identify the most appropriate model from a wide range of different techniques that suits best their experimental goals, practical considerations, and laboratory environment.

Declaration of conflicting interests

The author(s) declared no potential conflicts of interest with respect to the research, authorship, and/or publication of this article.

Author contributions

Dr Marbacher contributed to the study concept, screened titles and abstracts, analyzed the data, prepared the figures, obtained personal funding, and wrote the article. Dr Strange screened titles and abstracts, extracted full-text data, and prepared the tables. Drs Fandino and Frösén directed the project and helped to write the article.

ORCID iD

Fabio Strange https://orcid.org/0000-0002-6441-4398

Supplementary material

Supplementary material for this article is available online.

References

1. Marbacher S, Niemela M, Hernesniemi J, et al. Recurrence of endovascularly and microsurgically treated intracranial aneurysms-review of the putative role of aneurysm wall biology. *Neurosurg Rev* 2019; 42(1): 49–58.
2. Texakalidis P, Sweid A, Mouchtouris N, et al. Aneurysm formation, growth, and rupture: the biology and physics of cerebral aneurysms. *World Neurosurg* 2019; 130: 277–284.
3. Stehbens WE. Cerebral aneurysms of animals other than man. *J Pathol Bacteriol* 1963; 86: 160–168.
4. Muroi C, Hugelshofer M, Seehusen F, et al. Natural cerebral aneurysm and spontaneous subarachnoid hemorrhage in mammals other than man: is there a scope for comparative medicine? *World Neurosurg* 2019; 122: 384–389.
5. Hashimoto N, Handa H and Hazama F. Experimentally induced cerebral aneurysms in rats. *Surg Neurol* 1978; 10: 3–8.
6. Nuki Y, Tsou TL, Kurihara C, et al. Elastase-induced intracranial aneurysms in hypertensive mice. *Hypertension* 2009; 54: 1337–1344.
7. Stehbens WE. Chronic changes in the walls of experimentally produced aneurysms in sheep. *Surg Gynecol Obstet* 1979; 149: 43–48.
8. Tenjin H, Fushiki S, Nakahara Y, et al. Effect of Guglielmi detachable coils on experimental carotid artery aneurysms in primates. *Stroke* 1995; 26: 2075–2080.
9. Hashimoto N, Kim C, Kikuchi H, et al. Experimental induction of cerebral aneurysms in monkeys. *J Neurosurg* 1987; 67: 903–905.
10. Bouzeghrane F, Naggara O, Kallmes DF, et al. In vivo experimental intracranial aneurysm models: a systematic review. *AJNR Am J Neuroradiol* 2010; 31: 418–423.
11. Herrmann AM, Meckel S, Gounis MJ, et al. Large animals in neurointerventional research: a systematic review on models, techniques and their application in endovascular procedures for stroke, aneurysms and vascular malformations. *J Cereb Blood Flow Metab* 2019; 39: 375–394.
12. Moher D, Shamseer L, Clarke M, et al. Preferred reporting items for systematic review and meta-analysis protocols (PRISMA-P) 2015 statement. *Syst Rev* 2015; 4: 1.
13. German WJ and Black SP. Experimental production of carotid aneurysms. *New Eng J Med* 1954; 250: 104–106.
14. Varsos V, Heros RC, DeBrun G, et al. Construction of experimental "giant" aneurysms. *Surg Neurol* 1984; 22: 17–20.
15. Massoud TF, Guglielmi G, Ji C, et al. Experimental saccular aneurysms. I. Review of surgically-constructed models and their laboratory applications. *Neuroradiology* 1994; 36: 537–546.
16. Marbacher S, Marjamaa J, Abdelhameed E, et al. The Helsinki rat microsurgical sidewall aneurysm model. *J Vis Exp* 2014; 92: e51071.

17. Byrne JV, Hope JK, Hubbard N, et al. The nature of thrombosis induced by platinum and tungsten coils in saccular aneurysms. *AJNR Am J Neuroradiol* 1997; 18: 29–33.

18. Guglielmi G, Ji C, Massoud TF, et al. Experimental saccular aneurysms. II. A new model in swine. *Neuroradiology* 1994; 36: 547–550.

19. Yatomi K, Yamamoto M, Mitome-Mishima Y, et al. New experimental model of terminal aneurysms in Swine: technical note. *J Neurol Surg A Cent Eur Neurosurg* 2012; 73: 397–400.

20. Ding YH, Tieu T and Kallmes DF. Creation of sidewall aneurysm in rabbits: aneurysm patency and growth follow-up. *J Neurointerv Surg* 2014; 6(1): 29–31.

21. Turk AS, Aagaard-Kienitz B, Niemann D, et al. Natural history of the canine vein pouch aneurysm model. *AJNR Am J Neuroradiol* 2007; 28: 531–532.

22. Fingerhut AG and Alksne JF. Thrombosis of intracranial aneurysms. An experimental approach utilizing magnetically controlled iron particles. *Radiology* 1966; 86: 342–343.

23. Roach MR. A model study of why some intracranial aneurysms thrombose but others rupture. *Stroke* 1978; 9: 583–587.

24. Ebara M, Yuki I, Murayama Y, et al. A rabbit model for efficacy evaluation of endovascular coil materials. *Surg Neurol* 2009; 72: 620–627; discussion 627.

25. Abrahams JM, Forman MS, Grady MS, et al. Delivery of human vascular endothelial growth factor with platinum coils enhances wall thickening and coil impregnation in a rat aneurysm model. *AJNR Am J Neuroradiol* 2001; 22: 1410–1417.

26. Ohyama T, Nishide T, Iwata H, et al. Vascular endothelial growth factor immobilized on platinum microcoils for the treatment of intracranial aneurysms: experimental rat model study. *Neurol Med Chir (Tokyo)* 2004; 44: 279–285; discussion 286–287.

27. Anidjar S, Salzmann JL, Gentric D, et al. Elastase-induced experimental aneurysms in rats. *Circulation* 1990; 82: 973–981.

28. Cawley CM, Dawson RC, Shengelaia G, et al. Arterial saccular aneurysm model in the rabbit. *AJNR Am J Neuroradiol* 1996; 17: 1761–1766.

29. Cloft HJ, Altes TA, Marx WF, et al. Endovascular creation of an in vivo bifurcation aneurysm model in rabbits. *Radiology* 1999; 213: 223–228.

30. Altes TA, Cloft HJ, Short JG, et al. 1999 ARRS Executive Council Award. Creation of saccular aneurysms in the rabbit: a model suitable for testing endovascular devices. American Roentgen Ray Society. *AJR Am J Roentgenol* 2000; 174: 349–354.

31. Ding YH, Dai D, Lewis DA, et al. Can neck size in elastase-induced aneurysms be controlled? A retrospective study. *AJNR Am J Neuroradiol* 2006; 27: 1681–1684.

32. Ding YH, Danielson MA, Kadirvel R, et al. Modified technique to create morphologically reproducible elastase-induced aneurysms in rabbits. *Neuroradiology* 2006; 48: 528–532.

33. Ding YH, Dai D, Danielson MA, et al. Control of aneurysm volume by adjusting the position of ligation during creation of elastase-induced aneurysms: a prospective study. *AJNR Am J Neuroradiol* 2007; 28: 857–859.

34. Ding YH, Kadirvel R, Dai D, et al. Creation of bifurcation-type elastase-induced aneurysms in rabbits. *AJNR Am J Neuroradiol* 2013; 34: E19–E21.

35. Krings T, Moller-Hartmann W, Hans FJ, et al. A refined method for creating saccular aneurysms in the rabbit. *Neuroradiology* 2003; 45: 423–429.

36. Villano JS, Boehm CA, Carney EL, et al. Complications of elastase-induced arterial saccular aneurysm in rabbits: case reports and literature review. *Comp Med* 2012; 62: 480–486.

37. Hoh BL, Rabinov JD, Pryor JC, et al. A modified technique for using elastase to create saccular aneurysms in animals that histologically and hemodynamically resemble aneurysms in human. *Acta Neurochir (Wien)* 2004; 146: 705–711.

38. Moller-Hartmann W, Krings T, Stein KP, et al. Aberrant origin of the superior thyroid artery and the tracheoesophageal branch from the common carotid artery: a source of failure in elastase-induced aneurysms in rabbits. *AJR Am J Roentgenol* 2003; 181: 739–741.

39. Kainth D, Salazar P, Safinia C, et al. A modified method for creating elastase-induced aneurysms by ligation of common carotid arteries in rabbits and its effect on surrounding arteries. *J Vasc Interv Neurol* 2017; 9: 26–35.

40. Wang Y, Ma C, Xu N, et al. An improved elastase-based method to create a saccular aneurysm rabbit model. *Br J Neurosurg* 2013; 27: 779–782.

41. Hoh BL, Velat GJ, Wilmer EN, et al. A novel murine elastase saccular aneurysm model for studying bone marrow progenitor-derived cell-mediated processes in aneurysm formation. *Neurosurgery* 2010; 66: 544–550; discussion 550.

42. Ruzevick J, Jackson C, Pradilla G, et al. Aneurysm formation in proinflammatory, transgenic haptoglobin 2-2 mice. *Neurosurgery* 2013; 72: 70–76; discussion 76.

43. Dobashi H, Akasaki Y, Yuki I, et al. Thermoreversible gelation polymer as an embolic material for aneurysm treatment: a delivery device for dermal fibroblasts and basic fibroblast growing factor into experimental aneurysms in rats. *J Neurointerv Surg* 2013; 5: 586–590.

44. Fujiwara NH, Cloft HJ, Marx WF, et al. Serial angiography in an elastase-induced aneurysm model in rabbits: evidence for progressive aneurysm enlargement after creation. *AJNR Am J Neuroradiol* 2001; 22: 698–703.

45. Ding Y, Dai D, Kadirvel R, et al. Five-year follow-up in elastase-induced aneurysms in rabbits. *AJNR Am J Neuroradiol* 2010; 31: 1236–1239.

46. Lewis DA, Ding YH, Dai D, et al. Morbidity and mortality associated with creation of elastase-induced saccular aneurysms in a rabbit model. *AJNR Am J Neuroradiol* 2009; 30: 91–94.

47. Zeng Z, Kallmes DF, Durka MJ, et al. Hemodynamics and anatomy of elastase-induced rabbit aneurysm models: similarity to human cerebral aneurysms? *AJNR Am J Neuroradiol* 2011; 32: 595–601.

48. Kallmes DF, Fujiwara NH, Berr SS, et al. Elastase-induced saccular aneurysms in rabbits: a

dose-escalation study. *AJNR Am J Neuroradiol* 2002; 23: 295–298.

49. Aassar OS, Fujiwara NH, Marx WF, et al. Aneurysm growth, elastinolysis, and attempted doxycycline inhibition of elastase-induced aneurysms in rabbits. *J Vasc Interv Radiol* 2003; 14: 1427–1432.

50. Wang S, Dai D, Kolumam Parameswaran P, et al. Rabbit aneurysm models mimic histologic wall types identified in human intracranial aneurysms. *J Neurointerv Surg* 2018; 10: 411–415.

51. Abruzzo T, Shengelaia GG, Dawson RC 3rd, et al. Histologic and morphologic comparison of experimental aneurysms with human intracranial aneurysms. *AJNR Am J Neuroradiol* 1998; 19: 1309–1314.

52. Strother CM, Graves VB and Rappe A. Aneurysm hemodynamics: an experimental study. *AJNR Am J Neuroradiol* 1992; 13(4): 1089–1095.

53. Naggara O, Darsaut TE, Salazkin I, et al. A new canine carotid artery bifurcation aneurysm model for the evaluation of neurovascular devices. *AJNR Am J Neuroradiol* 2010; 31: 967–971.

54. Young PH and Yasargil MG. Experimental carotid artery aneurysms in rats: a new model for microsurgical practice. *J Microsurg* 1982; 3: 135–146.

55. Yang XJ, Li L and Wu ZX. A novel arterial pouch model of saccular aneurysm by concomitant elastase and collagenase digestion. *J Zhejiang Univ Sci B* 2007; 8: 697–703.

56. Macdonald RL, Mojtahedi S, Johns L, et al. Randomized comparison of Guglielmi detachable coils and cellulose acetate polymer for treatment of aneurysms in dogs. *Stroke* 1998; 29: 478–485; discussion 485–486.

57. Stehbens WE. Experimental production of aneurysms by microvascular surgery in rabbits. *Vasc Surg* 1973; 7: 165–175.

58. Ujiie H, Tachibana H, Hiramatsu O, et al. Effects of size and shape (aspect ratio) on the hemodynamics of saccular aneurysms: a possible index for surgical treatment of intracranial aneurysms. *Neurosurgery* 1999; 45: 119–129; discussion 129–130.

59. Miskolczi L, Guterman LR, Flaherty JD, et al. Saccular aneurysm induction by elastase digestion of the arterial wall: a new animal model. *Neurosurgery* 1998; 43: 595–600; discussion 600–601.

60. Nishikawa M, Yonekawa Y and Matsuda I. Experimental aneurysms. *Surg Neurol* 1976; 5: 15–18.

61. Young PH, Fischer VW, Guity A, et al. Mural repair following obliteration of aneurysms: production of experimental aneurysms. *Microsurgery* 1987; 8: 128–137.

62. Gao YZ, van Alphen HA and Kamphorst W. Observations on experimental saccular aneurysms in the rat after 2 and 3 months. *Neurol Res* 1990; 12: 260–263.

63. van Alphen HA, Gao YZ and Kamphorst W. An acute experimental model of saccular aneurysms in the rat. *Neurol Res* 1990; 12: 256–259.

64. Mucke T, Holzle F, Wolff KD, et al. Microsurgically induced pure arterial aneurysm model in rats. *Cent Eur Neurosurg* 2011; 72: 38–41.

65. Sekhar LN, Sclabassi RJ, Sun M, et al. Intra-aneurysmal pressure measurements in experimental saccular aneurysms in dogs. *Stroke* 1988; 19: 352–356.

66. Shin YS, Niimi Y, Yoshino Y, et al. Creation of four experimental aneurysms with different hemodynamics in one dog. *AJNR Am J Neuroradiol* 2005; 26: 1764–1767.

67. Boulos AS, Deshaies EM, Fessler RD, et al. A triple bifurcation aneurysm model for evaluating complex endovascular therapies in dogs. *J Neurosurg* 2005; 103: 739–744.

68. Massoud TF, Ji C, Guglielmi G, et al. Experimental models of bifurcation and terminal aneurysms: construction techniques in swine. *AJNR Am J Neuroradiol* 1994; 15: 938–944.

69. Forrest MD and O'Reilly GV. Production of experimental aneurysms at a surgically created arterial bifurcation. *AJNR Am J Neuroradiol* 1989; 10: 400–402.

70. Spetzger U, Reul J, Weis J, et al. Microsurgically produced bifurcation aneurysms in a rabbit model for endovascular coil embolization. *J Neurosurg* 1996; 85: 488–495.

71. Bavinzski G, al-Schameri A, Killer M, et al. Experimental bifurcation aneurysm: a model for in vivo evaluation of endovascular techniques. *Minim Invasive Neurosurg* 1998; 41: 129–132.

72. Sherif C, Marbacher S, Erhardt S, et al. Improved microsurgical creation of venous pouch arterial bifurcation aneurysms in rabbits. *AJNR Am J Neuroradiol* 2011; 32: 165–169.

73. Kirse DJ, Flock S, Teo C, et al. Construction of a vein-pouch aneurysm at a surgically created carotid bifurcation in the rat. *Microsurgery* 1996; 17: 681–689.

74. Nishikawa M, Smith RD and Yonekawa Y. Experimental intracranial aneurysms. *Surg Neurol* 1977; 7: 241–244.

75. Jiang YZ, Lan Q, Wang QH, et al. Creation of experimental aneurysms at a surgically created arterial confluence. *Eur Rev Med Pharmacol Sci* 2015; 19: 4241–4248.

76. Marbacher S, Erhardt S, Schlappi JA, et al. Complex bilobular, bisaccular, and broad-neck microsurgical aneurysm formation in the rabbit bifurcation model for the study of upcoming endovascular techniques. *AJNR Am J Neuroradiol* 2011; 32: 772–777.

77. Marbacher S, Tastan I, Neuschmelting V, et al. Long-term patency of complex bilobular, bisaccular, and broad-neck aneurysms in the rabbit microsurgical venous pouch bifurcation model. *Neurol Res* 2012; 34: 538–546.

78. Yapor W, Jafar J and Crowell RM. One-stage construction of giant experimental aneurysms in dogs. *Surg Neurol* 1991; 36: 426–430.

79. Ysuda R, Strother CM, Aagaard-Kienitz B, et al. A large and giant bifurcation aneurysm model in canines: proof of feasibility. *AJNR Am J Neuroradiol* 2012; 33: 507–512.

80. Sherif C, Herbich E, Plasenzotti R, et al. Very large and giant microsurgical bifurcation aneurysms in rabbits: Proof of feasibility and comparability using

computational fluid dynamics and biomechanical testing. *J Neurosci Methods* 2016; 268: 7–13.

81. Fahed R, Darsaut TE, Salazkin I, et al. Testing stenting and flow diversion using a surgical elastase-induced complex fusiform aneurysm model. *AJNR Am J Neuroradiol* 2017; 38: 317–322.

82. Darsaut TE, Bing F, Salazkin I, et al. Flow diverters failing to occlude experimental bifurcation or curved sidewall aneurysms: an in vivo study in canines. *J Neurosurg* 2012; 117: 37–44.

83. Darsaut TE, Bing F, Salazkin I, et al. Testing flow diverters in giant fusiform aneurysms: a new experimental model can show leaks responsible for failures. *AJNR Am J Neuroradiol* 2011; 32: 2175–2179.

84. Greim-Kuczewski K, Berenstein A, Kis S, et al. Surgical technique for venous patch aneurysms with no neck in a rabbit model. *J Neurointerv Surg* 2018; 10: 118–121.

85. Darsaut TE, Bing F, Salazkin I, et al. Flow diverters can occlude aneurysms and preserve arterial branches: a new experimental model. *AJNR Am J Neuroradiol* 2012; 33: 2004–2009.

86. Avery MB, Alaqeel A, Bromley AB, et al. A refined experimental model of fusiform aneurysms in a rabbit carotid artery. *J Neurosurg* 2018(1); 131: 88–95.

87. Yan L, Zhu YQ, Li MH, et al. Geometric, hemodynamic, and pathological study of a distal internal carotid artery aneurysm model in dogs. *Stroke* 2013; 44: 2926–2929.

88. Nakayama Y, Satow T, Funayama M, et al. Construction of 3 animal experimental models in the development of honeycomb microporous covered stents for the treatment of large wide-necked cerebral aneurysms. *J Artif Organs* 2016; 19: 179–187.

89. Krings T, Busch C, Sellhaus B, et al. Long-term histological and scanning electron microscopy results of endovascular and operative treatments of experimentally induced aneurysms in the rabbit. *Neurosurgery* 2006; 59: 911–923; discussion 923–924.

90. Dai D, Ding YH, Danielson MA, et al. Histopathologic and immunohistochemical comparison of human, rabbit, and swine aneurysms embolized with platinum coils. *AJNR Am J Neuroradiol* 2005; 26: 2560–2568.

91. Kallmes DF, Helm GA, Hudson SB, et al. Histologic evaluation of platinum coil embolization in an aneurysm model in rabbits. *Radiology* 1999; 213: 217–222.

92. Saqr KM, Rashad S, Tupin S, et al. What does computational fluid dynamics tell us about intracranial aneurysms? A meta-analysis and critical review. *J Cereb Blood Flow Metab*. Epub ahead of print 18 June 2019. DOI: 10.1177/0271678X19854640.

93. Raymond J, Darsaut T, Salazkin I, et al. Mechanisms of occlusion and recanalization in canine carotid bifurcation aneurysms embolized with platinum coils: an alternative concept. *AJNR Am J Neuroradiol* 2008; 29: 745–752.

94. Scholz M, Mucke T, During M, et al. Microsurgically induced aneurysm models in rats, part I: techniques and histological examination. *Minim Invasive Neurosurg* 2008; 51: 76–82.

95. Zanetti PH and Sherman FE. Experimental evaluation of a tissue adhesive as an agent for the treatment of aneurysms and arteriovenous anomalies. *J Neurosurg* 1972; 36: 72–79.

96. Frosen J, Marjamaa J, Myllarniemi M, et al. Contribution of mural and bone marrow-derived neointimal cells to thrombus organization and wall remodeling in a microsurgical murine saccular aneurysm model. *Neurosurgery* 2006; 58: 936–944; discussion 936–944.

97. Sadasivan B, Ma S, Dujovny M, et al. Use of experimental aneurysms to evaluate wrapping materials. *Surg Neurol* 1990; 34: 3–7.

98. O'Reilly GV, Utsunomiya R, Rumbaugh CL, et al. Experimental arterial aneurysms: modification of the production technique. *J Microsurg* 1981; 2: 219–223.

99. Ding YH, Tieu T and Kallmes DF. Creation of sidewall aneurysm in rabbits: aneurysm patency and growth follow-up. *J Neurointerv Surg* 2014; 6: 29–31.

100. Kerber CW and Buschman RW. Experimental carotid aneurysms: I. Simple surgical production and radiographic evaluation. *Invest Radiol* 1977; 12: 154–157.

101. Kallmes DF, Altes TA, Vincent DA, et al. Experimental side-wall aneurysms: a natural history study. *Neuroradiology* 1999; 41: 338–341.

102. Black SP and German WJ. Observations on the relationship between the volume and the size of the orifice of experimental aneurysms. *J Neurosurg* 1960; 17: 984–990.

103. Yoshino Y, Niimi Y, Song JK, et al. Preventing spontaneous thrombosis of experimental sidewall aneurysms: the oblique cut. *AJNR Am J Neuroradiol* 2005; 26: 1363–1365.

104. Becker TA, Preul MC, Bichard WD, et al. Preliminary investigation of calcium alginate gel as a biocompatible material for endovascular aneurysm embolization in vivo. *Neurosurgery* 2007; 60: 1119–1127; discussion 1127–1128.

105. Platz J, Guresir E, Seifert V, et al. Long-term effects of antiplatelet drugs on aneurysm occlusion after endovascular treatment. *J Neurointerv Surg* 2012; 4: 345–350.

106. Chalouhi N, Atallah E, Jabbour P, et al. Aspirin for the prevention of intracranial aneurysm rupture. *Neurosurgery* 2017; 64: 114–118.

107. Stehbens WE. In re: histological and morphologic comparison of experimental aneurysms with human intracranial aneurysms. *AJNR Am J Neuroradiol* 2000; 21: 1769–1773.

108. Raymond J, Berthelet F, Desfaits AC, et al. Cyanoacrylate embolization of experimental aneurysms. *AJNR Am J Neuroradiol* 2002; 23: 129–138.

109. Raymond J, Salazkin I, Metcalfe A, et al. Lingual artery bifurcation aneurysms for training and evaluation of neurovascular devices. *AJNR Am J Neuroradiol* 2004; 25: 1387–1390.

110. Nevzati E, Rey J, Coluccia D, Gruter BE, et al. Aneurysm wall cellularity affects healing after coil embolization: assessment in a rat saccular aneurysm model. *J Neurointerv Surg*. Epub ahead of print 23 December 2019. DOI: 10.1136/neurintsurg-2019-015335.

111. Marbacher S, Frosen J, Marjamaa J, et al. Intraluminal cell transplantation prevents growth and rupture in a model of rupture-prone saccular aneurysms. *Stroke* 2014; 45: 3684–3690.

112. Marbacher S, Marjamaa J, Bradacova K, et al. Loss of mural cells leads to wall degeneration, aneurysm growth, and eventual rupture in a rat aneurysm model. *Stroke* 2014; 45: 248–254.

113. Ding YH, Dai D, Lewis DA, et al. Can neck size in elastase-induced aneurysms be controlled? A prospective study. *AJNR Am J Neuroradiol* 2005; 26: 2364–2367.

114. Onizuka M, Miskolczi L, Gounis MJ, et al. Elastase-induced aneurysms in rabbits: effect of postconstruction geometry on final size. *AJNR Am J Neuroradiol* 2006; 27: 1129–1131.